OCEAN SURFACE WAVES: ATTENUATION AND A FIELD TEST OF DSA II

by

Alden Buffington Chace, Jr.

United States
Naval Postgraduate School

THESIS

OCEAN SURFACE WAVES:
ATTENUATION AND A FIELD TEST OF DSA II

by

Alden Buffington Chace, Jr.

October 1969

Ocean Surface Waves: Attenuation and a Field Test of DSA II

by

Alden Buffington Chace, Jr.
Lieutenant, United States Navy
B.S., United States Naval Academy, 1962

Submitted in partial fulfillment of the
requirements for the degree of

MASTER OF SCIENCE IN OCEANOGRAPHY

from the

NAVAL POSTGRADUATE SCHOOL
October 1969

ABSTRACT

Several models of ocean surface wave attenuation were employed in making hindcasts for comparison with spectra obtained from a wave recorder located at Point Sur, California. Quantitative decay models were reduced to common variables. The French Meteorological Service DSA II generation model was used.

The attenuation model which best fits the data obtained is $n = \exp(-20\ T^{-2}\ t)$, where n is a ratio of energy at the start of decay to that remaining afterwards, T is wave period in seconds, and t is decay duration in hours. The period range considered was 8.5 to 23.5 seconds.

TABLE OF CONTENTS

LIST OF ILLUSTRATIONS

TABLE OF SYMBOLS AND ABBREVIATIONS

Symbol	Definition	Unit
DSA	Spectro-angular density.	---
X	Incremental distance of generation or decay	naut. mile
L	Deep water wave length.	ft
L_s	Wave length at sensor position.	ft
T	Wave period.	sec
t	Time required for wave energy of a given period to travel a distance X. The duration interval for generation or decay.	hr
g	Acceleration of gravity.	$\frac{ft}{sec^2}$
W	Wind speed (nm/hr).	knots
θ	Angle between wind direction and direction of energy propagation under consideration. $0^o \leq \theta \leq 180^o$; $\theta = 180^o$ is an adverse wind.	degrees
f	Wave frequency.	hertz
ρ	Density of sea water (2.0).	$\frac{slugs}{ft^3}$
E	Total wave energy for band indicated.	ft^2
E(f)	Wave energy as a function of frequency.	ft^2
E(0)	Initial wave energy present in a band of periods at the start of an increment of generation or decay.	ft^2
E(X)	Wave energy in the same band of periods as E(0) after propagating a distance X in time t.	ft^2
R(0)	Initial energy density (French) proportional to (1/2) ρ g E(0). See Appendix A.	$\frac{centijoules}{cm^2}$

$R(X)$	Final energy density (French) at end of distance X. Corresponds to E(X).	$\frac{\text{centijoules}}{\text{cm}^2}$
n	Attenuation function = $\frac{E(X)}{E(0)} = \frac{R(X)}{R(0)}$.	---
α	Groen [1954] and [1950] attenuation coefficient.	$\text{meter}^{1/6}$
K	Paquin constant (1.26).	$\text{sec}^{-5/3}$
d	Depth of pressure sensor (65).	ft
$\frac{dl_0}{dl}$	Refraction coefficient. The ratio of orthogonal separation in deep water to that at the sensor location.	---
x	Incremental distance of generation or decay.	meters

ACKNOWLEDGMENTS

The author wishes to express his sincere appreciation to advisors Associate Professor J. B. Wickham, who originally suggested the topic, and Dr. T. Green III, both of whom provided immeasurable assistance of all types. I am indebted to Miss Diane Budde for color coding the wave propagation diagrams. My particular thanks are due to Dr. R. Gelci of the French Meteorological Service for several letters and publications on the subject of DSA II.

I. INTRODUCTION

Neither the magnitudes nor the mechanisms of ocean wave attenuation have been well determined for ocean surface waves with periods of 8.5 to 23.5 seconds. The standard wave forecasting method in the United States, for nearly 15 years, has been the Pierson, Neumann, and James [1955] method. The 'PNJ' technique allows for angular spreading but fails to consider mechanisms of attenuation.

Wave attenuation studies have been conducted using various methods of attack. Theoretical and experimental approaches lead to a variety of proposed mechanisms for the damping of wave energy. Wave forecasters have devised empirical methods of estimating loss of wave energy during propagation from a specified fetch area to an observation point.

The French DSA series of forecasting methods attempted to improve on the limited fetch methods of 'PNJ' by considering wave energy approaching the forecast point from several directions. The DSA method number two (DSA II) [Gelci, Cazale, and Vassal 1957] employs an attenuation model which allows for decay as a function of wave period, decay distance, and cross-wind condition. This method was developed in the North Atlantic Ocean. Field use in the Pacific Ocean provided an opportunity to evaluate DSA II under different geographical conditions.

The objectives of this thesis were two-fold. First, to test DSA II in a region in the Northeast Pacific extending roughly 2000 miles from Point Sur, California and, second, to attempt to evaluate some

of the proposed attenuation models. The method employed was comparison of hindcasts (made using DSA II) with analyzed wave records from Point Sur, California for January 1948.

II. ATTENUATION THEORIES AND MODELS

When ocean waves propagate out of a region of active generation a period of attenuation commences. It is generally believed that longer waves decrease in height more slowly than their shorter counterparts. The following mechanisms and experiments provide insight into the processes which may be involved.

A. PROPOSED MECHANISMS OF DECAY

1. Molecular Viscosity

Viscous dissipation has been suggested. However, it has been noted theoretically that viscous amplitude decay time for ocean waves varies as the square of wave length [Kinsman 1965]. Except for very minute ocean waves, such as parasitic capillaries, viscous decay is several orders of magnitude too small to explain observed decay.

2. Wave Breaking

Breaking of waves is a method of converting wave energy into turbulence. It is the most important mechanism in the generating area [Barnett 1966] and on the final beach but is rare elsewhere [Cartwright 1967]. Wave-wave interaction, as discussed below (II. A. 6.), may lead to breaking.

3. External Turbulence

Groen [1954] and Bowden [1950] ascribed wave damping primarily to externally caused turbulence. This turbulence is produced independently of the wave. An artificial "eddy vicsosity" may be used to deal with this mechanism as long as the size of turbulent eddies is small compared to the length of the waves [Barber and Ursell 1948].

Bowden assumed monochromatic significant waves. Groen dealt with wave spectra to arrive at an energy decay expression of the following form: $n = \exp - (\alpha x L^{-7/6})$. Here n is the ratio of energy at the start of a region of decay to that present at the end of the region of length x (meters); L is the deep water wave length in meters; α is Groen's attenuation coefficient in units of meter$^{1/6}$. The energies were in a band centered at wave length L.

Groen [1954, p. 7] stated that turbulence is frequency selective and attenuates the shorter period waves more rapidly. Thus it is better to employ wave spectra rather than assume, as a representative system, only the significant waves present.

4. Air Resistance

Darbyshire [1957] examined air resistance and concluded that it did not provide a dominant mechanism of decay since he found actual attenuation to be independent of wind speed for a following wind.

Phillips [1966, p. 148] concluded that the condition of θ greater than 90° results in a very weak coupling between wind and swell which leads to an exponential form of decay. Here, θ is the angle between the wind direction and the direction of energy propagation under consideration. He suggested that the attenuation is proportional to COS θ.

5. Parasitic Capillaries

Phillips [1966, p. 134] discussed capillary waves which tend to form as standing waves in advance of the sharp crests of short gravity waves due to local surface tension effects. The capillary waves are small enough to cause viscous attenuation to

be significant. This mechanism is important in the case of steep gravity waves of length 5 to 30 cm. Therefore it is significant in small lakes but probably not in the ocean where most energy is concentrated in lower frequencies.

6. Wave-Wave Interaction

Barnett [1966] suggested that, once the wind has ceased its active generation, the spectrum looses energy mainly through wave-wave interactions. Gelci and Cazale [1962, p. 30] have developed a model (DSA V) to consider losses due to the interaction between wave trains. DSA II does not consider this effect. Yet the decay observed in DSA V is quite similar to that resulting in DSA II. Gelci (personal correspondence) reports that wave-wave interaction does not significantly affect waves with a period of 14 seconds or greater.

The details of the wave-wave interaction mechanism are complex, but the effect is the transfer of energy from three active wave components to a fourth, passive component. The magnitude of the effect appears to be comparable to wave generation processes [Barnett 1966]. For a typical fully developed spectrum, energy is transferred from a broad mid-frequency band to both higher and lower frequencies. The energy transferred to higher frequencies could be lost via breaking and viscosity.

7. Scattering Due to Turbulence

Phillips [1961] proposed that some ocean turbulence is generated by gravity waves. This is a type of turbulence not included in the externally caused turbulence (see II. A. 3.). Phillips [1959] developed a theory to explain attenuation and directional scattering

of surface gravity waves which appears to result from interaction between wave turbulence and wave motion. His conclusion was that scattering would predominate over viscous attenuation for wave lengths greater than about 3 meters (periods of 1.4 sec). It is not certain that this would be a significant effect since viscous effects themselves are small for the 8.5 to 23.5 second periods covered by this thesis. Phillips' theory results in the following model for which values are tabulated in Appendix C: $n = \exp -(0.0087\ T^{-5/3}\ t)$.

B. EXPERIMENTS

The first serious application of modern analysis techniques to ocean waves occurred in the early 1940's [Cartwright 1967]. It was discovered that random fluctuations in sea level from wave records can be resolved with spectral analysis into the sum of a number of quasi-periodic oscillations of various frequencies or periods. Most of the wave measurements made during the next ten years were used to develop wave generation models and parameters for energy-density spectra.

1. San Clemente Study

During the 1950's, Munk, Miller, Snodgrass, and Barber [1963] examined wave energy received at San Clemente, California from storm waves generated in distant regions of the North Pacific and in the Southern Ocean. They detected significant amounts of energy only at frequencies below 5.0×10^{-2} hz (periods larger than 20 sec). Wave energy at higher frequencies was heavily attenuated somewhere along the great circle path [Cartwright 1967]. This result was used in justification of hindcasting waves on the basis of surface winds within 2000 nm of Point Sur for this thesis.

2. New Zealand to Alaska Attenuation Study

Munk and his colleagues set up one of the most ambitious series of measurements in the history of oceanography [Snodgrass et al. 1966]. During the summer of 1963 they tracked swell along a great circle path from New Zealand to Alaska using six observation stations. At frequencies above 7.0×10^{-2} hz (period 14.3 sec) there was a tendency for spectral energy to decrease at a rate of 1/10 db per degree along the great circle path. This is equivalent to the equation:

$$n = \exp\left[-(0.011 \text{ sec}^{-1} \text{ hr}^{-1})\ T\ t\right].$$

Comparative values are presented in Appendix C. Below 7.2×10^{-2} hz the energy either remained constant or increased. Cartwright [1967] indicated that the major result of this experiment was that attenuation above 5.0×10^{-2} hz (period 20 sec) in the first 20^{o} or so from the generation area was much greater than that observed over the rest of the path to Alaska.

3. Small Amplitude Deep Water Wave Study

Carswell [1968], of the Naval Postgraduate School, looked at very small waves (frequencies 2 to 2.4 hz) in a lake. Following a suggestion of Professor J. B. Wickham, Carswell used his data to fit an f^{N} exponential decay function. An N of three gave the best fit and resulted in the following: $n = \exp\left[-\left(5 \frac{\text{sec}^3}{\text{nm}}\right) f^3\ X\right]$. Here, f is frequency in hertz; X is decay distance in nautical miles. This expression was modified to the following equivalent form for evaluation in this thesis:

$$n = \exp\left[-\left(7.575 \frac{\text{sec}^2}{\text{hr}}\right) T^{-2}\ t\right].$$

4. Spectro-Angular Attenuation

DSA II has its own attenuation function, which was developed for use in the North Atlantic and is applicable where the angle between the wind direction in the decay region and the direction of energy propagation (θ) exceeds 60^{o} or wind velocity (W) is not greater than ten knots. This function is:

$$n = \exp\left[-\left\{100 + 0.38416\left(\frac{W^4}{T^2}\right)\sin^2\left(\frac{3}{4}\theta - 45^{o}\right)\right\}\sec^2 \text{ hr}^{-1}\ t\ T^{-2}\right].$$

When θ does not exceed 60^{o} and W is greater than ten knots DSA II assumes no decay. Gelci (personal correspondence) points out that this is nearly true for an isolated component and DSA II neglected "interferential decay" due to multiple wave trains. The case of θ no greater than 60^{o} and W in excess of 10 knots is taken care of by either maintaining steady-state or generation as applicable for the wave period under consideration.

5. Eddy Viscosity Application

Groen and Dorrestein [1950] evaluated the attenuation coefficient (α), in the equation previously presented (II. A. 3.), to get an empirical value (8.5×10^{-4} meter$^{1/6}$). Their equation has been modified to a more convenient form for this thesis:

$$n = \exp\left[-(1.92 \times 10^{-2} \text{ sec}^{4/3} \text{ hr}^{-1})\ t\ T^{-4/3}\right].$$

6. Laboratory Underwater Turbulence Study

Paquin [1968] studied the effect of grid-generated underwater turbulence on small waves (1.2 to 12.3 hz) in a wave tank. His results showed that turbulent attenuation would have the following form: $n = \exp\left[-2\left\{\frac{2\ K\ f^{1/3}}{g}\right\}X\right]$, where K is a constant ($1.26 \text{ sec}^{-5/3}$);

X is a decay distance (in units compatible with g); g is gravitational acceleration; and f is frequency in hz. This was converted to variables convenient to DSA II as shown below:

$$n = \exp\left[-(4.55 \times 10^{3}\ \text{sec}^{-2/3}\ \text{hr}^{-1})\ t\ T^{2/3}\right].$$

A table of values is not provided as this model is not applicable to the ocean. The values of n approach zero very rapidly.

III. DATA AND ANALYSIS

Air Weather Service, Northern Hemisphere Historical Weather Maps were used to select a time interval with desirable conditions for this study during the period for which wave records were available. The interval 5 January 1948 through 12 January 1948 was used because of a cyclonic disturbance located approximately 1500 nm northwest of Point Sur. This disturbance, which varied in strength, produced time varying wave energy.

Microfilm reproductions of United States Weather Bureau, North American Surface Weather Charts were used as a source of wind-field data. Only actual ship wind reports were used and given a minor amount of smoothing. The result was a realistic wind field comparable to that employed for DSA II by the French Meteorological Service.

Wave records were obtained from a Mark III pressure wave sensor installed near the bottom at Point Sur, California by the Department of Engineering, University of California as part of an investigation of surface waves conducted for the Bureau of Ships, United States Navy. The sensor was located in sixty-five feet of water [Isaacs and Saville 1949] on a bearing of 240° true from Point Sur. The recorder operated at a tape speed of three inches per minute for 20 minutes out of each eight hour interval [Wiegel 1949].

A. HINDCAST PREPARATION

Unlike the 'PNJ' method DSA II requires no fetch definitions but instead considers the action of the space- and time-varying winds

on each wave component. Therefore results are much less subject to the interpretation of the hindcaster.

The procedure for hindcast preparation is summarized by the following expression:

$$E_s = \left\{ \sum_{Az} \int_0^t G \, dt \left[2 \; C \right] \left[\frac{dl_0}{dl} \right] \right\} \left[\frac{L_0}{L_s} \right]$$

where E_s is the hindcasted energy in feet square for a given period band at the sensor position off Point Sur; $\sum_{Az}$ is a summation over the various azimuths of energy approach to Point Sur; G is the generation and decay function which, when integrated over duration, yields the energy in centijoules/cm^2 arriving from a specified azimuth; 2 compensates for a 20^o separation between azimuths instead of the 10^o specified in DSA II; C is a unit conversion (see Appendix A) from centijoules/cm^2 to the feet squared energy representation; $\frac{dl_0}{dl}$ is the correction for refraction; and $\frac{L_0}{L_s}$ corrects for shoaling.

1. Wind-Field Plot

Ship wind reports were transferred from microfilm to a plot as shown in Figure (1), which illustrates typical data density for the six hourly wind-field. Due to the limited detail of the wind-field, azimuths from Point Sur were positioned every 20^o true instead of every ten degrees as called for in DSA II. Azimuths were limited to the north by Point Reyes which bears 325^o true from Point Sur. Bearing 320^o true from Point Sur is a 300 ft shoal off Point Reyes which refracts waves whose period is greater than 11 seconds.

2. Propagation Diagrams

The propagation diagram is an extremely valuable means of establishing the wind history of waves arriving at an observation

Figure 1. Sample Wind Field Plot

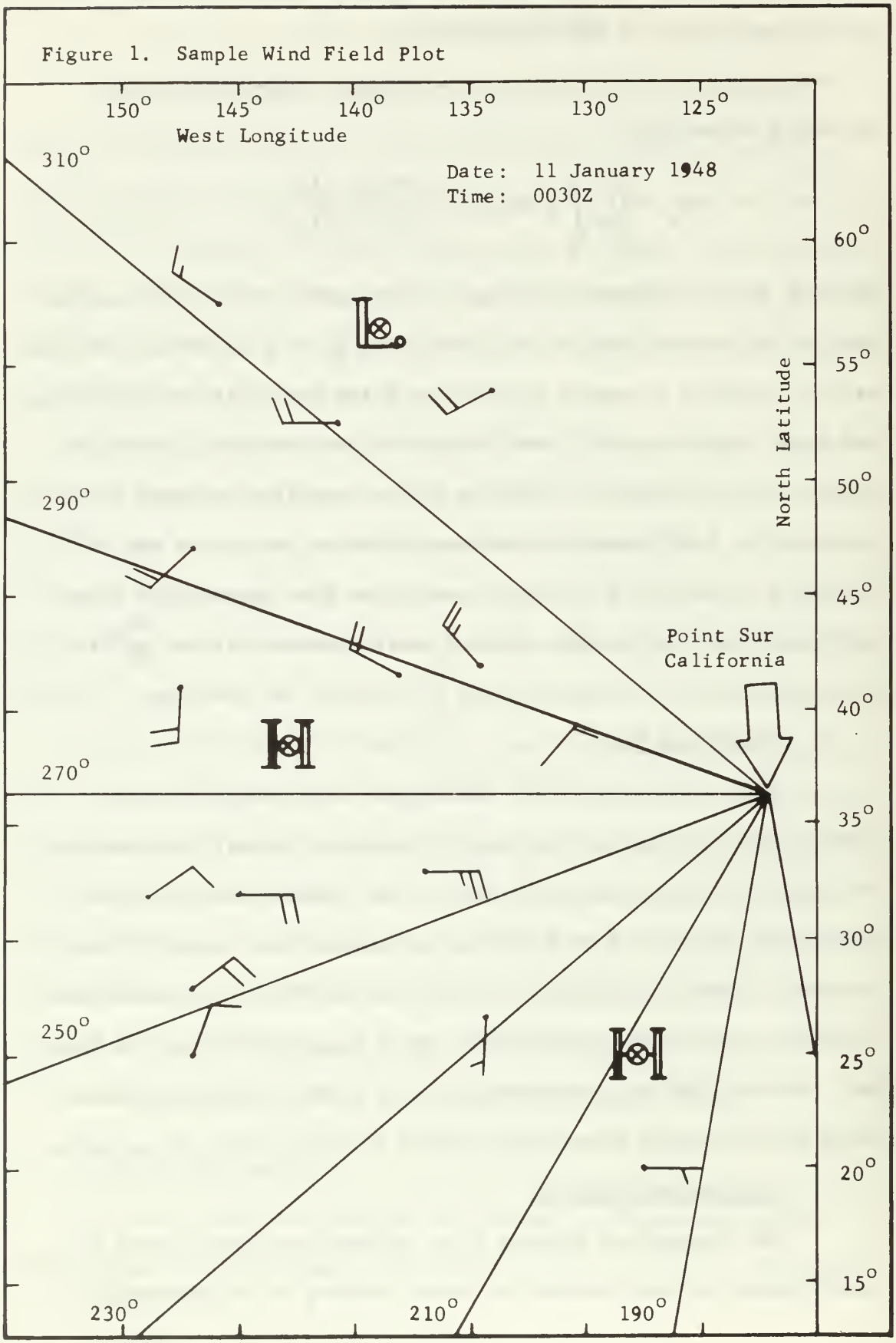

point along a particular azimuth. Figure (2) depicts a portion of one diagram. Actual diagrams were plotted continuously for the interval of 5 through 12 January 1948 to a range of 2000 nm from Point Sur.

Each propagation diagram gives the wind conditions as a function of time and distance from the observation point along one azimuth in the wind field plot. For each increment of range (100 nm) and time (6 hrs) both θ and W were plotted. Here, θ is the angle between the wind direction and the direction of energy propagation along an azimuth and W is the wind velocity in knots. Isotachs were contoured every five knots of W. Wind directions were color coded into the following DSA II categories:

Description	θ or W Limits
Generating	$\theta \leq 20^{\circ}$
Favorable	$20^{\circ} < \theta \leq 60^{\circ}$
Favorable-Fair	$60^{\circ} < \theta \leq 90^{\circ}$
Contrary-Fair	$90^{\circ} < \theta \leq 120^{\circ}$
Contrary	$120^{\circ} < \theta \leq 180^{\circ}$
Calm	$W \leq 10$ kts

3. Energy Computation

Wave record availability within each eight hour interval dictated hindcast times. DSA II is designed to consider waves whose central periods are 20, 14, 10, and 7 seconds respectively. The 7 second waves were not used as they were obscured by hydrodynamic filtering and noise on the wave records.

A propagation line overlay was prepared on the basis of the group velocity of the three wave bands considered (see Figure 3).

Figure 2. Sample Propagation Diagram.

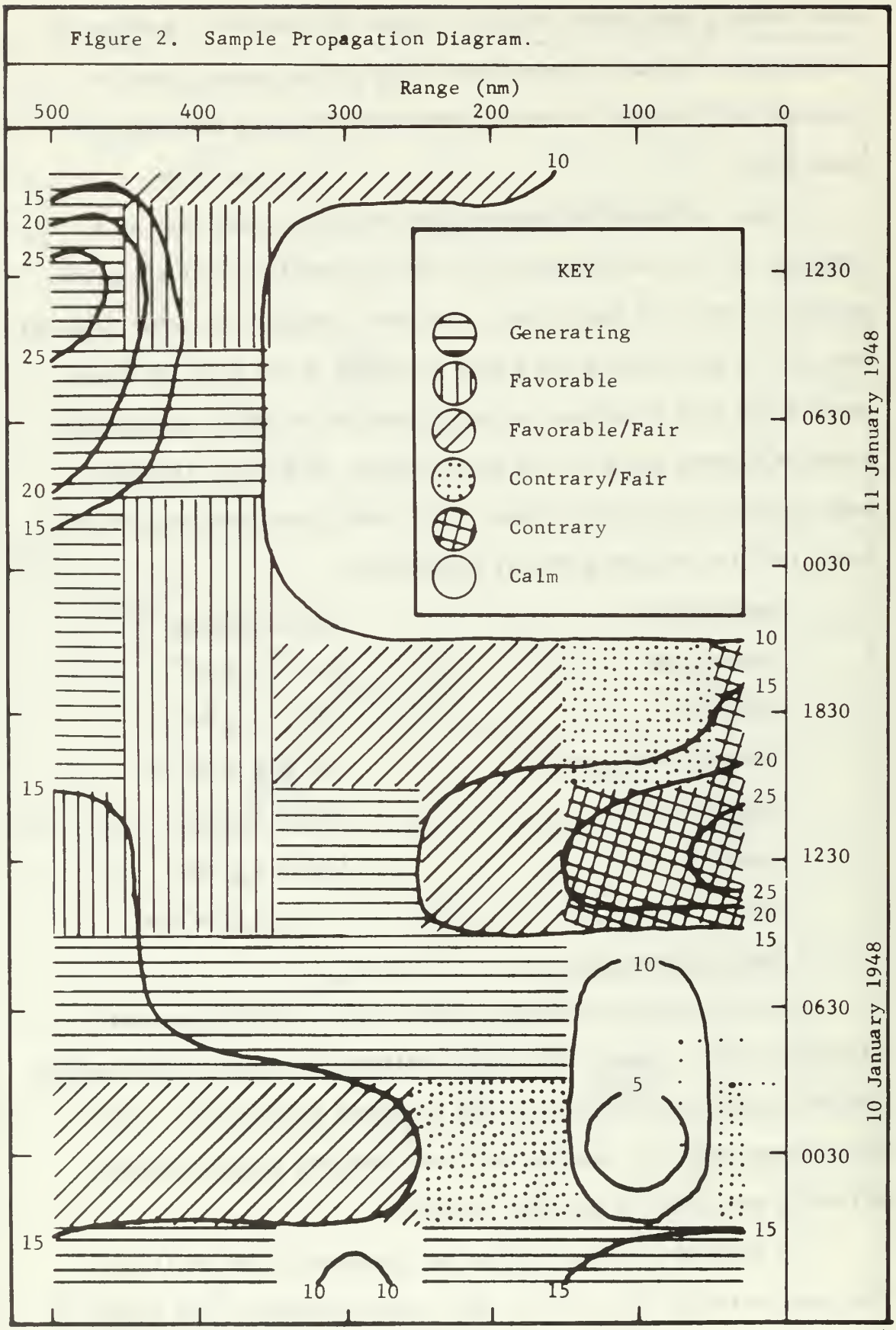

Figure 3. Propagation Line Overlay

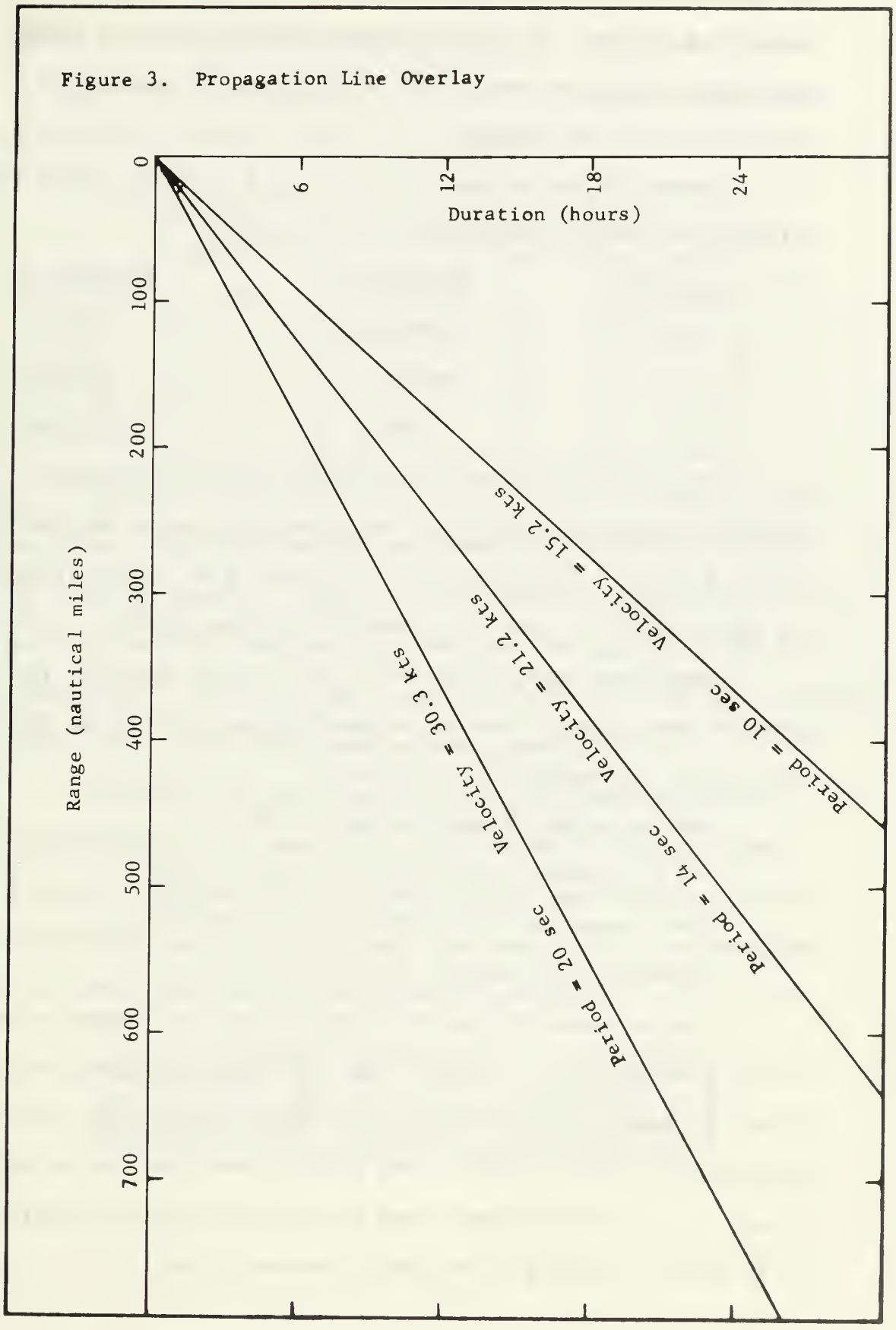

The advantages of the propagation diagram in combination with the overlay are evident. The corresponding ranges and times of each wave-energy packet are shown, and a hindcast can be computed for any given time on the diagram.

Generation was presumed to occur when $\theta \leqq 60^{o}$ and one of the following minimum W conditions was met or exceeded:

T (sec)	Generating θ	Favorable θ
20	40/45 kts	45 kts
14	30/35 kts	35 kts
10	25 kts	25/30 kts

When minimum generating or favorable winds were present the DSA II generation diagram for the appropriate period was entered with θ, W, and t. Subsequent intervals with $\theta \leqq 60^{o}$ either increased the energy density or left it unchanged depending upon W.

When θ was greater than 60^{o} or $W \leqq 10$ knots decay was presumed to occur. One of the four attenuation models below was then employed for the appropriate conditions:

Unmodified DSA II equation (see II. B. 4.).

DSA II equation with 1/10th of actual duration.

DSA II equation with 1/100th of actual duration.

Carswell decay function (see II. B. 3.).

This stepwise process was continued until the energy arrived at the observation point. Due to the large nearly stationary high pressure system to the southwest all hindcasted wave energy came from azimuths 270^{o}, 290^{o}, and 310^{o}. The reported winds were not strong enough at any of the hindcast times to generate waves with a period of 20 seconds according to the DSA II generation model.

The refraction coefficients (dl_0/dl) below were applied to the energy arriving from the various azimuths [Wiegel 1964, chapter 7]. The coefficient (dl_0/dl) is the ratio of orthogonal separation in deep water to that at the sensor location.

Azimuth	Wave Period (sec)	
	10 sec	14 sec
310^o	1.00	0.95
290^o	1.05	0.83
270^o	0.99	0.66

Within each period band the energy from the various azimuths was summed. The DSA II method considered azimuths of wave approach for every ten degrees. However in this problem the azimuths were 20^o apart and therefore the energy in each band was doubled to obtain the correct total. The resulting energy density in each band was converted to the feet squared representation (see Appendix A).

The arriving energy was corrected for shoaling through multiplication by the appropriate shoaling factor (L_0/L_s) below, where L_0 is deep water wave length and L_s is wave length in 65 feet of water (at the sensor position). The result is E_s for comparison to the observed value of E at the sensor position.

Period (sec)	10	14	20
Shoaling Factor	1.38	1.68	2.34

B. ANALYSIS OF WAVE RECORDS

A grid overlay was used to sample the analogue wave records at two-second intervals. This provided a time series of 512 data points per 20 minute wave record. The data points were read in arbitrary units and converted to feet of head. The mean reading was computed and subtracted from each value, the result being a series of zero mean.

Fourier amplitudes (coefficients) were obtained from the raw data using subroutine RHARM on the Naval Postgraduate School IBM 360 computer. RHARM is based upon the fast Fourier transform developed by Cooley and Tukey [1965]. The amplitudes were squared and summed into the following period bands:

DSA II Wave Description	Period (sec)	Band Limits (sec)	Bandwidth (sec)
Long	20	16.5-23.5	7
Medium	14	11.5-16.5	5
Short	10	8.5-11.5	3

The energy in each band is multiplied by $COSH^2 (2\pi d/L_s)$ [Wiegel 1964, Appendix 1] to obtain the energy at the surface, where L_s is the wave length at the sensor position and d is the depth of the pressure sensor (65 ft). The resulting energy is the observed energy for comparison to the hindcasted energy.

IV. GENERATION

Two assumptions were made that affect the amount of energy generated. First, the reported wind field was presumed to represent the actual winds present at a constant reporting height above the water suitable for use with DSA II. Second, the DSA II generation model was presumed to be correct and was used throughout so that decay parameters could be varied.

The first assumption was examined to define the effect of errors in the wind field. The following table indicates the approximate percentage error in wave energy which would result from a reported "generating" wind being 10% higher than the actual wind for a duration of 10 hours.

Actual Wind (kts)	Reported Wind (kts)	Period		
		Long	Medium	Short
25.0	27.5	0	0	211
30.0	33.0	0	∞	25
35.0	38.5	0	130	23
40.0	44.0	∞	75	10
45.0	49.5	105	30	3

If the reported wind is considered as a mean for the six hour period, then speed variations during the interval would tend to make the hindcasted energy too small. The effect of this phenomena seems to be minor.

It is apparent that a prerequisite for this type of study is an accurately defined wind field.

V. SUMMARY OF RESULTS

Figure (4) presents the results of the analyses done using the unmodified DSA II equation. The line marked "equal values" represents the position that should be occupied by all points if generation, decay and wind-field were correct and no scatter existed. This line is shown on each figure as a reference since various scales are used for the hindcast energy depending on its magnitude.

The DSA II equation led to hindcasts that, with the exception of two points, were zero. It was concluded that this model provided too rapid an energy decay if the generation function is appropriate.

Figure (5) shows the effect of using the DSA II decay equation with duration reduced to 1/10th of the actual duration. This was the best set of hindcasts made. Four of the five points farthest from the equal value line came from two hindcast times only six hours apart. This makes it appear that the reported wind-field for this area may have been stronger than the actual wind-field.

Figure (6) is the final hindcast made with a form of the DSA II equation. One hundredth of the duration was used in the DSA II equation and the hindcasts are generally too large.

A decay model slightly more rapid than the DSA II equation with 1/10th duration would give the best results as far as general magnitude is concerned. The DSA II decay showed a good balance as far as period is concerned. No one band of periods forms a predominant grouping away from the line of equal values.

Figure 4. Observed Energy vs Hindcast Energy
Using DSA II Decay Equation

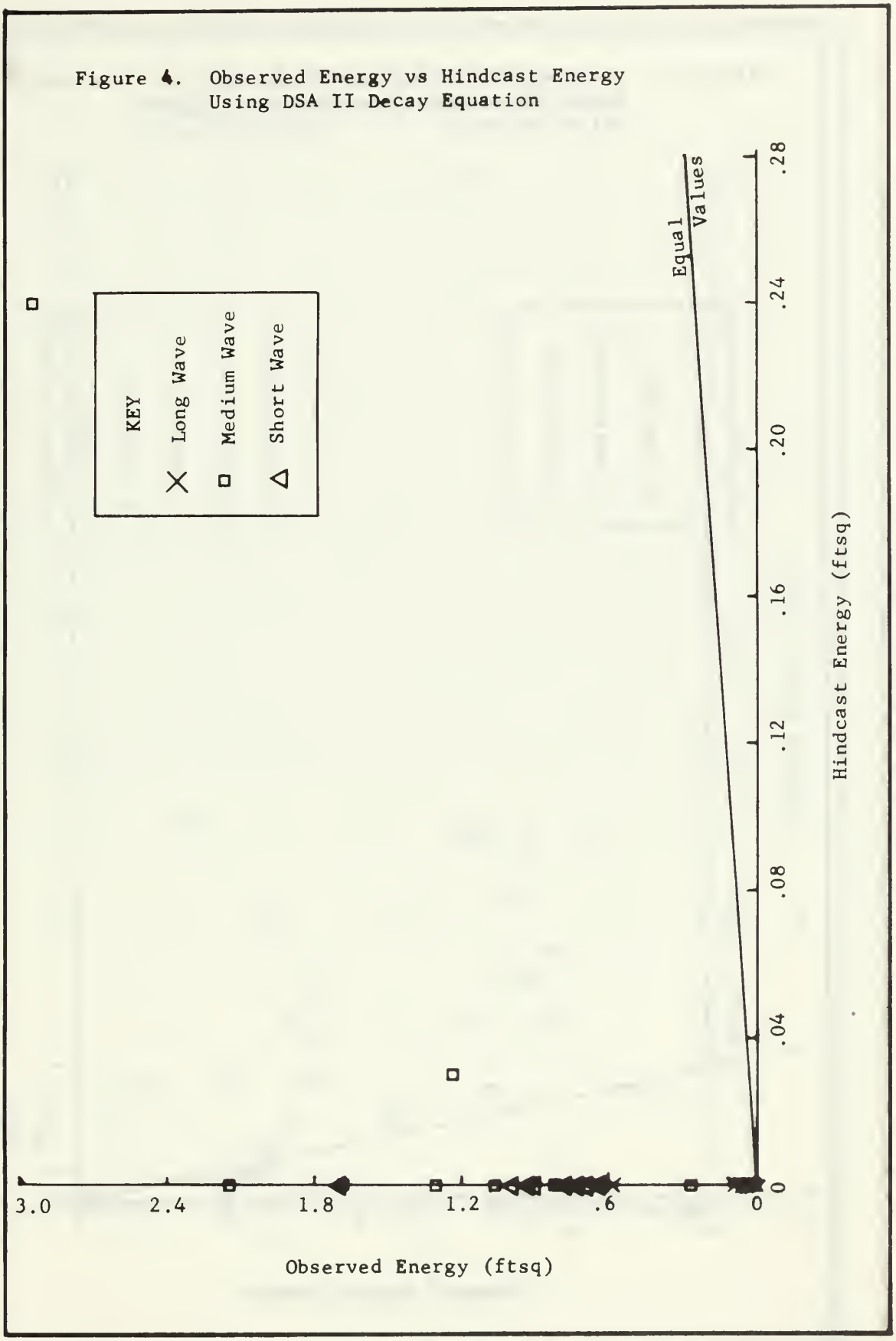

Figure 5. Observed Energy vs Hindcast Energy Using DSA II Decay Equation with 1/10th Actual Duration

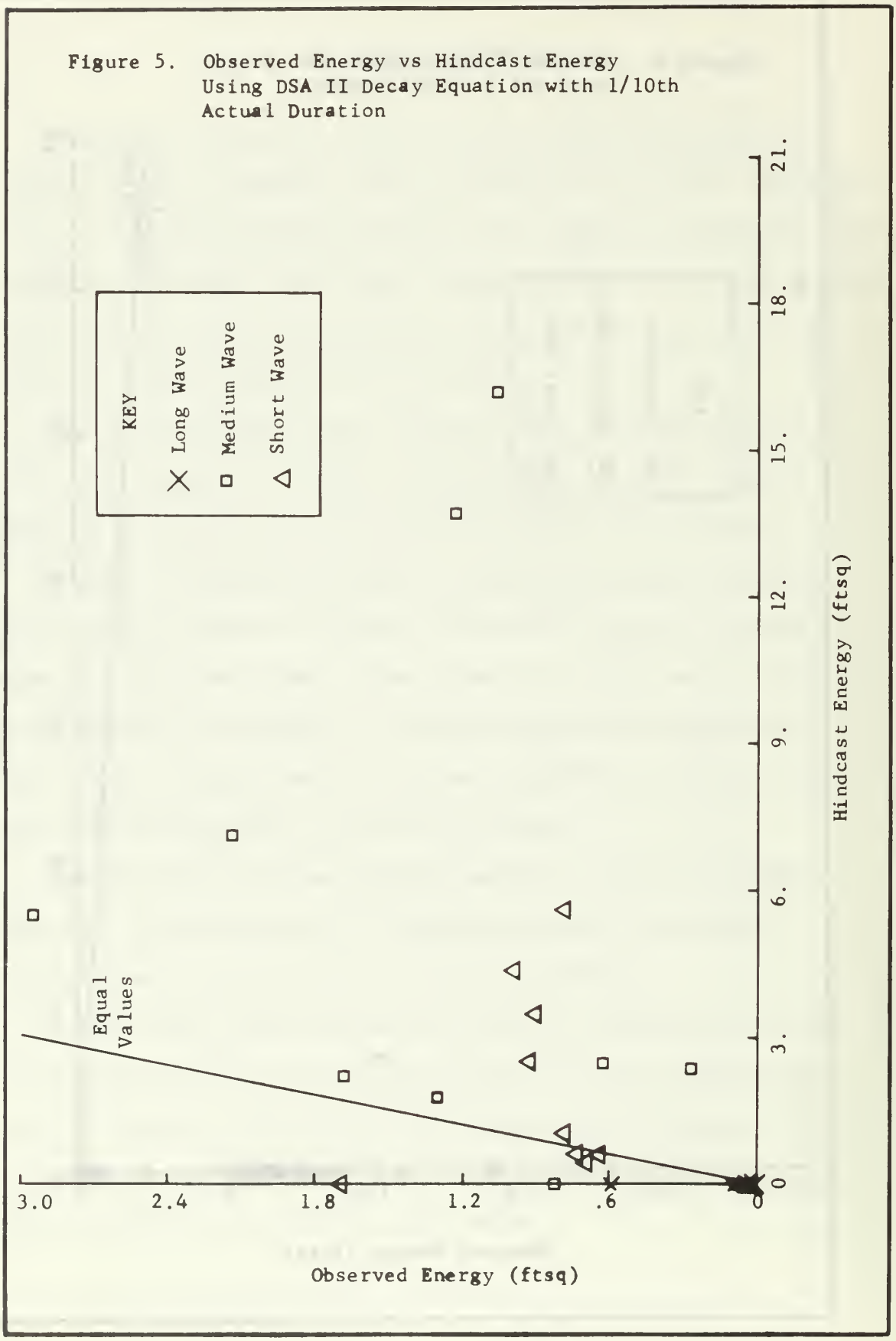

Figure 6. Observed Energy vs Hindcast Energy Using DSA II Decay Equation with 1/100th Actual Duration

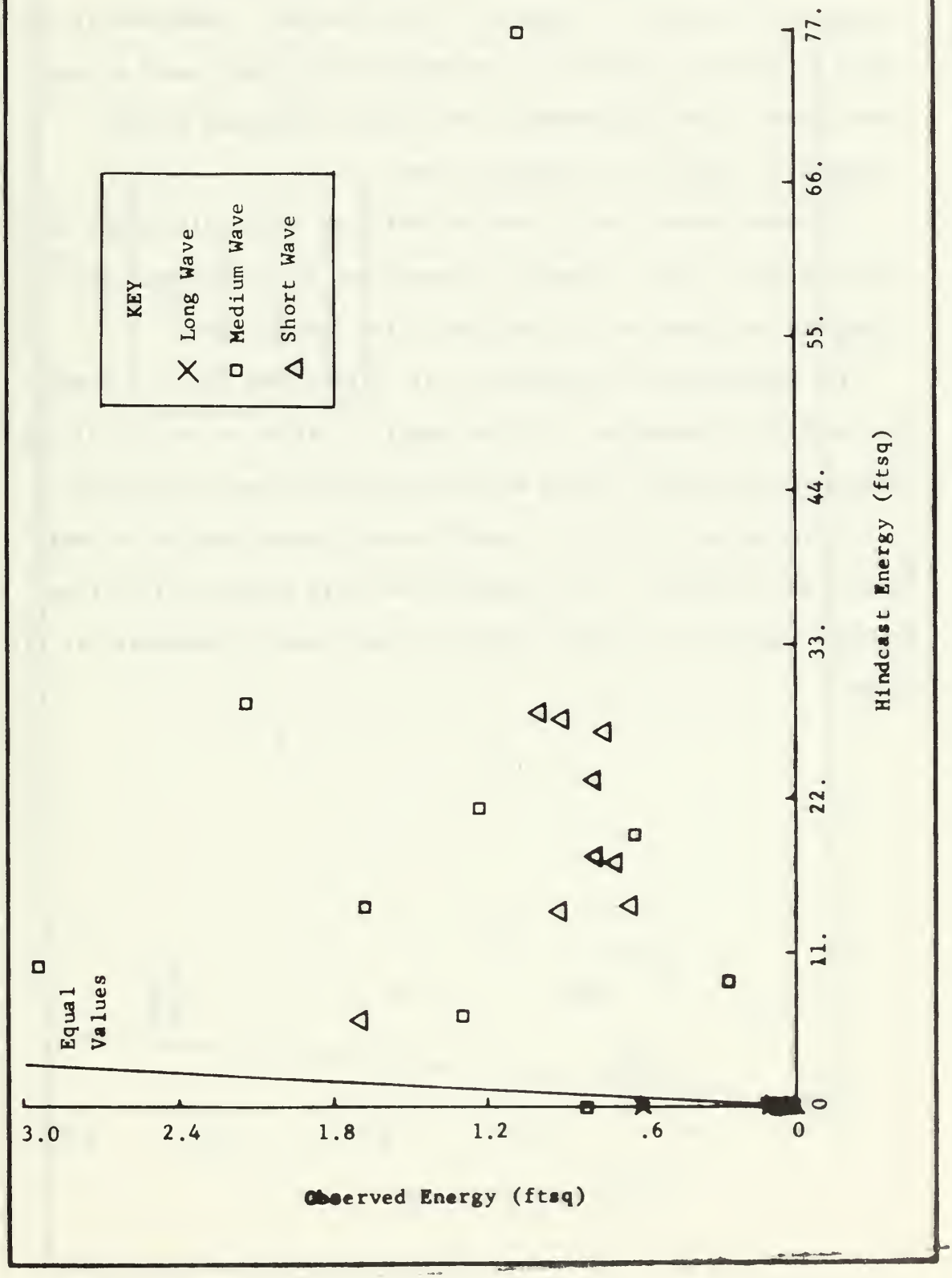

Figure (7) presents hindcasts made with Carswell decay. Like the DSA II equation, decay is modeled as a function of exp $[-(T^{-2})]$. The difference is the removal of the wind dependent term, which did not significantly degrade the quality of the hindcast. Snodgrass et al. [1966, p. 493] also observed in the Pacific Ocean that swell attenuation seems to be independent of the winds encountered during propagation outside the generating area.

The Groen decay function and the Phillips' scattering model were not used since visual inspection showed that both would make the hindcasts too large due to their very slow rate of decay.

The model based on Snodgrass et al. [1966] (see II. B. 2.) was not used for hindcasting. In this model, n varies as exp [-(T)] and thus attenuates small period waves more rapidly than is observed.

No energy was hindcast in the 20 second period band but a small amount was observed. It is probable that this energy arrived from distant regions in a manner similar to that noted by Snodgrass et al. [1966].

Figure 7. Observed Energy vs Hindcast Energy
Using Carswell Decay

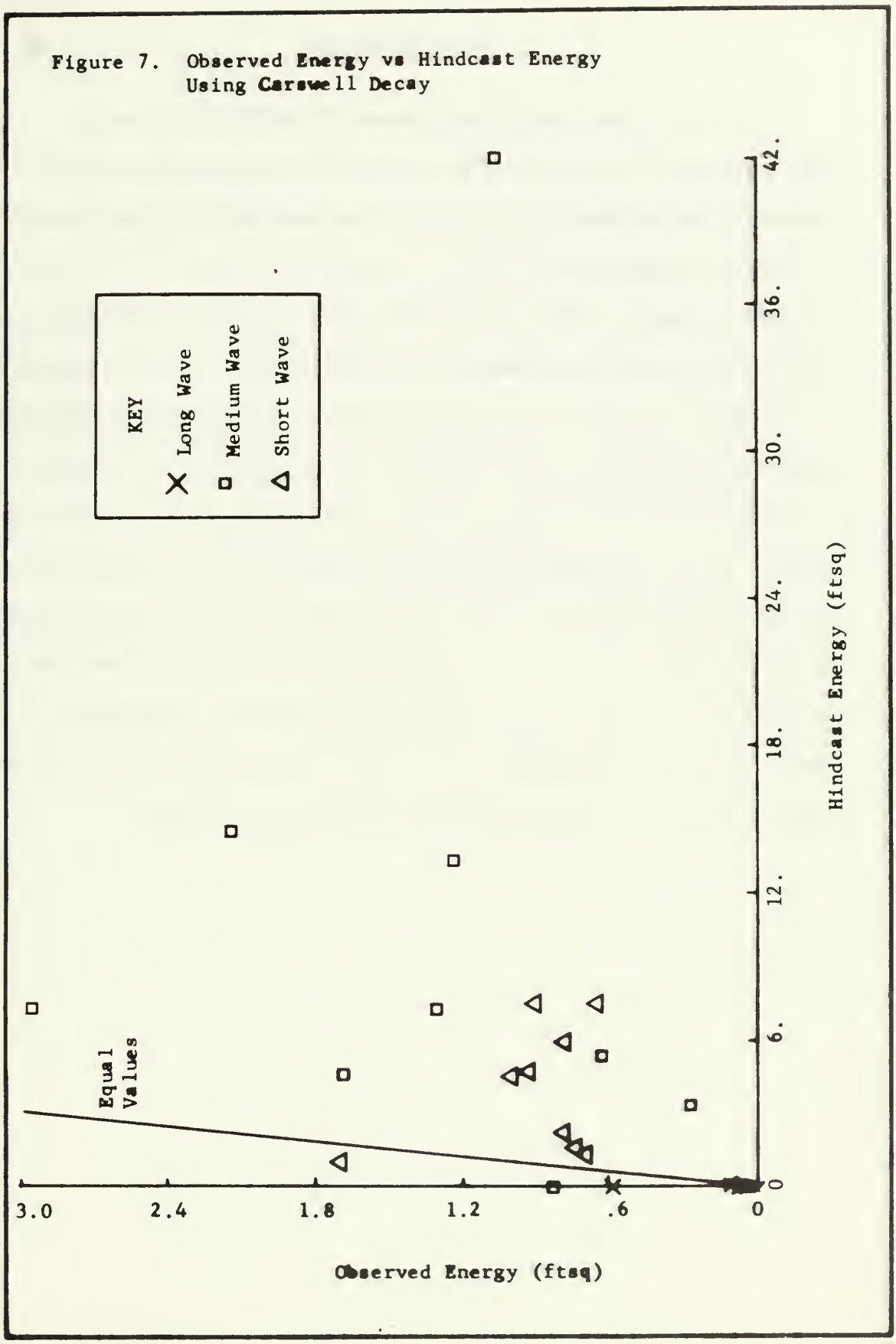

VI. CONCLUSIONS

The attenuation model which best fits the data obtained is $n = \exp(-20\ T^{-2}\ t)$, where n is a ratio of energy at the start of decay to that remaining afterwards, T is wave period in seconds, and t is decay duration in hours.

The advantage of a wind dependent term, as used in DSA II, in the decay model is unclear from the data obtained.

It was not possible to relate attenuation models to theories of decay in the ocean in this thesis.

Future work should employ a more detailed and more precise wind field. Also it is possible to reduce the influence of the generation model through analysis. Recent innovations in computer prepared wind field products may be a partial answer to the wind-field problem. Density of reporting ships has also increased since 1948 which is an important gain. Knowledge of the rate of ocean wave attenuation may provide the key to understanding the mechanisms of decay.

APPENDIX A

EQUATION OF ENERGY REPRESENTATIONS

The French Meteorological Service representation of energy as R(X) in centijoules/cm^2 can be converted to the amplitude squared notation of E(X) in ft^2 using the following: $R(X) = k \frac{1}{2} \rho g E(X)$ where ρg (sea water) is 64 lb/ft^3 and k is a constant unit conversion. Introducing appropriate unit conversions provides the following:

$$[E(X)ft^2] = \left[64 \frac{lb}{ft^3}\right]^2 \left[R(X) \frac{\text{centijoules}}{cm^2}\right] \left[\frac{\text{joule}}{10^2 \text{ centijoules}}\right]$$

$$\left[\frac{10^4 cm^2}{meter^2}\right] \left[\frac{0.0929 \text{ meter}^2}{ft^2}\right] \left[\frac{0.7376 \text{ ft-lb}}{\text{joule}}\right]$$

$E(X)ft^2 = 0.214\ R(X)$ centijoules/cm^2.

APPENDIX B

TABULAR DISPLAY OF SPECTRAL COMPONENTS

All dates refer to January 1948. Values given are energy in units of feet squared within the period band indicated.

1. Observation.
2. Hindcast using unmodified DSA II equation.
3. Hindcast using DSA II equation with 1/10th of actual duration.
4. Hindcast using DSA II equation with 1/100th of actual duration.
5. Hindcast using Carswell decay function.

1. Observation.

Date/Time	Period		
	Long	Medium	Short
07/1610	0.05	0.83	1.70
07/2215	0.59	1.31	0.65
08/0415	0.05	2.96	0.93
08/1015	0.06	1.24	0.79
08/1615	0.09	2.15	0.91
09/1000	0.03	1.69	1.00
10/1645	0.02	1.07	0.79
11/1615	0.03	0.63	0.74
12/1045	0.00	0.27	0.70

2. Hindcast using unmodified DSA II equation.

Date/Time	Period		
	Long	Medium	Short
07/1610	0.0	0.0	0.0
07/2215	0.0	0.0	0.0
08/0415	0.0	0.24	0.0
08/1015	0.0	0.03	0.0
08/1615	0.0	0.0	0.0
09/1000	0.0	0.0	0.0
10/1645	0.0	0.0	0.0
11/1615	0.0	0.0	0.0
12/1045	0.0	0.0	0.0

3. Hindcast using DSA II equation with 1/10th of actual duration.

Date/Time	Period		
	Long	Medium	Short
07/1610	0.0	0.0	0.0
07/2215	0.0	1.80	0.62
08/0415	0.0	5.49	2.52
08/1015	0.0	13.70	5.60
08/1615	0.0	7.13	3.46
09/1000	0.0	2.22	4.36
10/1645	0.0	16.17	1.03
11/1615	0.0	2.49	0.61
12/1045	0.0	2.35	0.44

4. Hindcast using DSA II equation with 1/100th of actual duration.

Date/Time	Period		
	Long	Medium	Short
07/1610	0.0	0.0	6.49
07/2215	0.0	6.54	14.63
08/0415	0.0	10.08	14.08
08/1015	0.0	21.55	17.93
08/1615	0.0	29.05	27.90
09/1000	0.0	14.42	28.15
10/1645	0.0	77.00	23.45
11/1615	0.0	19.50	26.91
12/1045	0.0	9.08	17.68

5. Hindcast using Carswell decay function.

Date/Time	Period		
	Long	Medium	Short
07/1610	0.0	0.0	0.95
07/2215	0.0	7.26	7.39
08/0415	0.0	7.30	4.68
08/1015	0.0	13.29	5.87
08/1615	0.0	14.51	7.44
09/1000	0.0	4.51	4.44
10/1645	0.0	41.92	2.21
11/1615	0.0	5.32	1.53
12/1045	0.0	3.28	1.21

APPENDIX C

ATTENUATION MODEL TABLES

1. Carswell Attenuation Function.
2. Groen Attenuation Function.
3. New Zealand - Alaska Attenuation Observations.
4. Phillips' Scattering Decay.

1. Carswell attenuation function.

Values of n are presented as functions of period (T) and decay duration (t). Carswell attenuation was applied when neither favorable nor generating winds of greater than 10 knots were reported.

t (hours)	Period		
	Long	Medium	Short
1/2	0.99	0.98	0.96
1	0.98	0.96	0.93
2	0.96	0.93	0.86
5	0.91	0.82	0.68
10	0.82	0.67	0.47
20	0.68	0.46	0.22
30	0.57	0.31	0.10
50	0.39	0.14	0.02

2. Groen attenuation function.

Values of n are presented as functions of period (T) and decay duration (t). This function was not used since it was apparent by inspection that the resulting hindcasts would be much too large.

t (hours)	Period		
	Long	Medium	Short
1/2	1.00	1.00	1.00
1	1.00	1.00	1.00
2	1.00	1.00	1.00
5	1.00	1.00	1.00
10	1.00	0.99	0.99
20	0.99	0.99	0.98
30	0.99	0.98	0.97
50	0.98	0.97	0.96

3. New Zealand - Alaska attenuation observations.

Values of n are presented as functions of period (T) and decay duration (t). This function is slightly more rapid in its attenuation of energy than the Carswell model. Compared to the results of this study decay is of the right order of magnitude. However, the frequency distribution does not appear correct. This study shows that short waves attenuate more rapidly than medium waves rather than as shown below.

t (hours)	Period	
	Medium	Short
1/2	0.9259	0.9465
1	0.8573	0.8958
2	0.7349	0.8025
5	0.4630	0.5770
10	0.2144	0.3329
20	0.0460	0.1108
30	0.0099	0.0369
50	0.0004	0.0041

4. Phillips Scattering Decay

Values of n are presented as functions of period (T) and decay duration (t). This function was not used for hindcasts since, by inspection, the rate of attenuation it models is much slower than that actually observed.

t (hours)	Period		
	Long	Medium	Short
1/2	1.0000	1.0000	0.9999
1	0.9999	0.9999	0.9998
2	0.9999	0.9998	0.9996
5	0.9997	0.9995	0.9991
10	0.9994	0.9989	0.9981
20	0.9988	0.9979	0.9963
30	0.9982	0.9968	0.9944
50	0.9970	0.9947	0.9907

REFERENCES CITED

Barber, N. F. and Ursell, F., "The Generation and Propagation of Ocean Waves and Swell," Phil. Trans. Roy. Soc. (London) A, v. 240, p. 527-560, 24 February 1948.

Barnett, T. P., On the Generation, Dissipation and Prediction of Ocean Wind Waves, Ph.D. Thesis, University of California, San Diego, Univ. Microfilms, Ann Arbor, Michigan (No. 67-6155), 1966.

Bowden, K. F., "The Effect of Eddy Viscosity on Ocean Waves," The Philosophical Magazine, series 7, v. 41, p. 907-917, September 1950.

Carswell, M. S., Attenuation of Surface Waves in Deep Water, MS Thesis, Naval Postgraduate School, Monterey, California, December 1968.

Cartwright, D. E., "Modern Studies of Wind-Generated Ocean Waves," Contemp. Phys., v. 8, no. 2, p. 171-183, March 1967.

Cooley, J. W. and Tukey, J. W., "An Algorithm for the Machine Calculation of Complex Fourier Series," Mathematics of Computations, v. 19, p. 297, April 1965.

Darbyshire, J., "Attenuation of Swell in the North Atlantic Ocean," Quar. J. Roy. Met. Soc., v. 83, no. 357, p. 351-359, 1957.

Gelci, R. and Cazalé, H., "Une Équation Synthétique de L'Evolution de L'Etat de La Mer," Journal de Méchanique et de Physique de L'Atmosphere, series II, no. 16, p. 15-41, October-December 1962.

Gelci, R., Cazalé, H., and Vassal, J., "Prevision de la Houle, La Methode des Densities Spectro-Angulaires," Bulletin d'Information du Comité Central d'Oceanographie et d'Etude des Côtes, series IX, no. 8, p. 416-435, September-October 1957.

Groen, P., "On the Behavior of Gravity Waves in a Turbulent Medium, with Application to the Decay and Apparent Period Increase of Swell," Netherlands. Meterologisch Instituut, Mededeelingen en Verhandelingen, series A, no. 63, p. 5-23, 1954.

Groen, P. and Dorrestein, R., "Ocean Swell: Its Decay and Period Increase," Nature, v. 165, no. 4194, p. 445-447, 18 March 1950.

Isaacs, J. D. and Saville, T., Jr., "A Comparison Between Recorded and Forecast Waves on the Pacific Coast," Ocean Surface Waves, Annals of the New York Academy of Sciences, v. 51, art. 3, p. 502-510, 13 May 1949.

Kinsman, B., Wind Waves; Their Generation and Propagation on the Ocean Surface, p. 501, Prentice-Hall, Inc., 1965.

Munk, W. H., and others, "Directional Recording of Swell from Distant Storms," Phil. Trans. Roy. Soc. (London) A, v. 255, no. 1062, p. 505-584, 1963.

Paquin, J. E., A Laboratory Experiment on Surface Wave Attenuation Due to Underwater Turbulence, MS Thesis, Naval Postgraduate School, Monterey, California, December 1968.

Pierson, W. J., Jr., Neumann, G., and James, R. W., Practical Methods for Observing and Forecasting Ocean Waves by Means of Wave Spectra and Statistics., p. 80-137, U. S. Navy Hydrographic Office Pub. No. 603, 1955.

Phillips, O. M., The Dynamics of the Upper Ocean, p. 134-154, Cambridge University Press, 1966.

Phillips, O. M., "A Note of the Turbulence Generated by Gravity Waves," J. of Geophysical Res., v. 66, no. 9, p. 2889-2893, September 1961.

Phillips, O. M., "The Scattering of Gravity Waves by Turbulence," J. of Fluid Mech., v. 5, no. 2, art. 12, p. 177-192, 1959.

Snodgrass, F. E., and others, "Propagation of Ocean Swell Across the Pacific," Phil. Trans. Roy. Soc. (London) A, v. 259, p. 431-497, 1966.

Wiegel, R. L., "An Analysis of Data from Wave Recorders on the Pacific Coast of the United States," Amer. Geoph. Union Trans., v. 30, no. 5, p. 701, October 1949.

Wiegel, R. L., Oceanographical Engineering, p. 516-524, Prentice-Hall, Inc., 1964.

REFERENCES CITED

Barber, N. F. and Ursell, F., "The Generation and Propagation of Ocean Waves and Swell," Phil. Trans. Roy. Soc. (London) A, v. 240, p. 527-560, 24 February 1948.

Barnett, T. P., On the Generation, Dissipation and Prediction of Ocean Wind Waves, Ph.D. Thesis, University of California, San Diego, Univ. Microfilms, Ann Arbor, Michigan (No. 67-6155), 1966.

Bowden, K. F., "The Effect of Eddy Viscosity on Ocean Waves," The Philosophical Magazine, series 7, v. 41, p. 907-917, September 1950.

Carswell, M. S., Attenuation of Surface Waves in Deep Water, MS Thesis, Naval Postgraduate School, Monterey, California, December 1968.

Cartwright, D. E., "Modern Studies of Wind-Generated Ocean Waves," Contemp. Phys., v. 8, no. 2, p. 171-183, March 1967.

Cooley, J. W. and Tukey, J. W., "An Algorithm for the Machine Calculation of Complex Fourier Series," Mathematics of Computations, v. 19, p. 297, April 1965.

Darbyshire, J., "Attenuation of Swell in the North Atlantic Ocean," Quar. J. Roy. Met. Soc., v. 83, no. 357, p. 351-359, 1957.

Gelci, R. and Cazalé, H., "Une Équation Synthétique de L'Evolution de L'Etat de La Mer," Journal de Méchanique et de Physique de L'Atmosphere, series II, no. 16, p. 15-41, October-December 1962.

Gelci, R., Cazalé, H., and Vassal, J., "Prevision de la Houle, La Methode des Densities Spectro-Angulaires," Bulletin d'Information du Comité Central d'Oceanographie et d'Etude des Côtes, series IX, no. 8, p. 416-435, September-October 1957.

Groen, P., "On the Behavior of Gravity Waves in a Turbulent Medium, with Application to the Decay and Apparent Period Increase of Swell," Netherlands. Meterologisch Instituut, Mededeelingen en Verhandelingen, series A, no. 63, p. 5-23, 1954.

Groen, P. and Dorrestein, R., "Ocean Swell: Its Decay and Period Increase," Nature, v. 165, no. 4194, p. 445-447, 18 March 1950.

Isaacs, J. D. and Saville, T., Jr., "A Comparison Between Recorded and Forecast Waves on the Pacific Coast," Ocean Surface Waves, Annals of the New York Academy of Sciences, v. 51, art. 3, p. 502-510, 13 May 1949.

Kinsman, B., Wind Waves; Their Generation and Propagation on the Ocean Surface, p. 501, Prentice-Hall, Inc., 1965.

Munk, W. H., and others, "Directional Recording of Swell from Distant Storms," Phil. Trans. Roy. Soc. (London) A, v. 255, no. 1062, p. 505-584, 1963.

Paquin, J. E., A Laboratory Experiment on Surface Wave Attenuation Due to Underwater Turbulence, MS Thesis, Naval Postgraduate School, Monterey, California, December 1968.

Pierson, W. J., Jr., Neumann, G., and James, R. W., Practical Methods for Observing and Forecasting Ocean Waves by Means of Wave Spectra and Statistics., p. 80-137, U. S. Navy Hydrographic Office Pub. No. 603, 1955.

Phillips, O. M., The Dynamics of the Upper Ocean, p. 134-154, Cambridge University Press, 1966.

Phillips, O. M., "A Note of the Turbulence Generated by Gravity Waves," J. of Geophysical Res., v. 66, no. 9, p. 2889-2893, September 1961.

Phillips, O. M., "The Scattering of Gravity Waves by Turbulence," J. of Fluid Mech., v. 5, no. 2, art. 12, p. 177-192, 1959.

Snodgrass, F. E., and others, "Propagation of Ocean Swell Across the Pacific," Phil. Trans. Roy. Soc. (London) A, v. 259, p. 431-497, 1966.

Wiegel, R. L., "An Analysis of Data from Wave Recorders on the Pacific Coast of the United States," Amer. Geoph. Union Trans., v. 30, no. 5, p. 701, October 1949.

Wiegel, R. L., Oceanographical Engineering, p. 516-524, Prentice-Hall, Inc., 1964.

INITIAL DISTRIBUTION LIST

		No. Copies
1.	Defense Documentation Center Cameron Station Alexandria, Virginia 22314	20
2.	Library, Code 0212 Naval Postgraduate School Monterey, California 93940	2
3.	Oceanographer of the Navy The Madison Building 732 N. Washington Street Alexandria, Virginia 22314	1
4.	Dr. T. Green III Department of Meteorology University of Wisconsin Madison, Wisconsin 57306	3
5.	Associate Professor J. B. Wickham Department of Oceanography Naval Postgraduate School Monterey, California 93940	3
6.	Dr. R. Gelci E. E. R. M./M. M. 196 rue de l' Universite Paris (VIIe) France	1
7.	Department of Oceanography Code 58 Naval Postgraduate School Monterey, California 93940	3
8.	Dr. T. Laevastu Fleet Numerical Weather Facility Naval Postgraduate School Monterey, California 93940	1
9.	Lieutenant A. B. Chace, Jr., USN USS HARDHEAD (SS 365) FPO New York, N. Y. 09501	1
10.	Associate Professor J. J. von Schwind Department of Oceanography Naval Postgraduate School Monterey, California 93940	1

11. Lieutenant Commander R. E. Ettle, USCG 1
Coast Guard Oceanographic Unit
Building 159-E
Navy Yard Annex
Washington, D. C. 20390

Security Classification

DOCUMENT CONTROL DATA - R & D

(Security classification of title, body of abstract and indexing annotation must be entered when the overall report is classified)

1. ORIGINATING ACTIVITY (Corporate author)	2a. REPORT SECURITY CLASSIFICATION
Naval Postgraduate School Monterey, California 93940	Unclassified
	2b. GROUP

3. REPORT TITLE

Ocean Surface Waves: Attenuation and a Field Test of DSA II

4. DESCRIPTIVE NOTES (Type of report and, inclusive dates)

Master's Thesis; October 1969

5. AUTHOR(S) (First name, middle initial, last name)

Alden Buffington Chace, Jr.

6. REPORT DATE	7a. TOTAL NO. OF PAGES	7b. NO. OF REFS
October 1969	52	22

8a. CONTRACT OR GRANT NO.	9a. ORIGINATOR'S REPORT NUMBER(S)
b. PROJECT NO.	
c.	9b. OTHER REPORT NO(S) (Any other numbers that may be assigned this report)
d.	

10. DISTRIBUTION STATEMENT

This document has been approved for public release and sale; its distribution is unlimited.

11. SUPPLEMENTARY NOTES	12. SPONSORING MILITARY ACTIVITY
	Naval Postgraduate School Monterey, California

13. ABSTRACT

Several models of ocean surface wave attenuation were employed in making hindcasts for comparison with spectra obtained from a wave recorder located at Point Sur, California. Quantitative decay models were reduced to common variables. The French Meteorological Service DSA II generation model was used.

The attenuation model which best fits the data obtained is $n = \exp(-20\ T^{-2}\ t)$, where n is a ratio of energy at the start of decay to that remaining afterwards, T is wave period in seconds, and t is decay duration in hours. The period range considered was 8.5 to 23.5 seconds.

DD FORM 1 NOV 65 1473 (PAGE 1)

S/N 0101-807-6811

Security Classification

A-31408

14 KEY WORDS	LINK A		LINK B		LINK C	
	ROLE	WT	ROLE	WT	ROLE	WT
Wave forecasting						
Wave decay						
DSA II						